VERSITA

Acta Geophysica
vol. 59, no. 1, Feb. 2011, pp. 183-204
DOI: 10.2478/s11600-010-0035-4

Estimation of Global Lightning Activity and Observations of Atmospheric Electric Field

Marek GOŁKOWSKI[1], Marek KUBICKI[2], Morris COHEN[3], Andrzej KUŁAK[4], and Umran S. INAN[3,5]

[1]Department of Electrical Engineering, University of Colorado Denver, Denver, CO, USA, e-mail: mark.golkowski@ucdenver.edu

[2]Institute of Geophysics, Polish Academy of Sciences, Warszawa, Poland e-mail: swider@igf.edu.pl (corresponding author)

[3]Department of Electrical Engineering, Stanford University, Stanford, CA, USA e-mails: mcohen@stanford.edu, inan@stanford.edu

[4]Astronomical Observatory, Jagiellonian University, Kraków, e-mail: radiol1@wp.pl; Department of Electronics, Academy of Mining and Metallurgy, Kraków, Poland

[5]Department of Electrical Engineering, Koç University Sariyer, Istanbul, Turkey

A b s t r a c t

Variations in the global atmospheric electric circuit are investigated using a wide range of globally spaced instruments observing VLF (~10 kHz) waves, ELF (~300 Hz) waves, Schumann resonances (4-60 Hz), and the atmospheric fair weather electric field. For the ELF/VLF observations, propagation effects are accounted for in a novel approach using established monthly averages of lightning location provided by the Lightning Image Sensor (LIS) and applying known frequency specific attenuation parameters for daytime/nighttime ELF/VLF propagation. Schumann resonances are analyzed using decomposition into propagating and standing waves in the Earth-ionosphere waveguide. Derived lightning activity is compared to existing global lightning detection networks and fair weather field observations. The results suggest that characteristics of lightning discharges vary by region and may have diverse effects upon the ionospheric potential.

Key words: global electric circuit, lightning discharges, ELF/VLF waves, Schumann resonances.

1. INTRODUCTION

The relationship between atmospheric currents and ionospheric potentials on a planetary scale is known as the global electric circuit. The global nature of the phenomena were first prominently documented in the reproducible worldwide diurnal variation of electric potential in the lower atmosphere. Wilson (1921) proposed a connection between the variation of atmospheric potential and thunderstorm activity in which the latter plays the role as a generator and current source. Although the global electric circuit has been the subject of study for almost 100 years, many questions remain and even fundamental assertions are often contended. While in the last few decades many authors have asserted that global thunderstorms and lightning directly drive the global circuit (Rycroft *et al*. 2000, Kartalev *et al*. 2006), several recent works suggest a contrary view. Rycroft *et al.* (2007) employed circuit simulation software to conclude that lightning discharges only contribute to ~1% of ionospheric potential changes and Williams and Sátori (2004) emphasize the importance of electrified shower clouds. It is worthy to note that Wilson (1921) initially postulated the importance of both ***thunderclouds and shower clouds*** although for many years the latter assertion was often overlooked. It is clear that the link between the DC phenomena of the equipotential global ionosphere and the AC phenomena of lightning discharges and their related effects are still poorly understood.

One of the challenges in investigating the global electric circuit is the difficulty in obtaining simultaneous measurements on a global scale. Observations of the "fair-weather" electric field as a measure of ionospheric potential have been recorded for many years but the notion of an equipotential global ionosphere is often muddled by effects of cosmic rays, energetic particle precipitation (Rycroft *et al.* 2000) and aerosol content in the stratosphere and troposphere (Tinsley and Zhou 2006). Even greater uncertainty exists in quantitative evaluation of global lightning activity despite recent technological advances in this area. The Optical Transient Detector (OTD) onboard the MicroLab-1 satellite and its successor, the Lightning Image Sensor (LIS) onboard the TRMM Observatory, have extended lightning detection into space (Christian *et al.* 2003). Both instruments detect lightning flashes optically with high efficiency but are limited to observing a finite viewing area providing global coverage only with multiple passes. Thus, although both LIS and OTD instruments provide extremely valuable long term averages of lightning frequency and distribution, they are unable to quantify lightning activity at any given instant.

Quantification of global lightning activity using radio measurements often involves the ELF and VLF bands because of the low attenuation and long distance propagation of lightning induced radiation at these frequencies.

In the ELF band, Schumann resonances are correlated with global lightning activity (Füllekrug and Fraser Smith 1996), but the determination of lightning location from Schumann resonances alone is difficult and requires special analysis (Kułak *et al.* 2006). Global lightning location networks in the VLF band have been constructed of which the World Wide Lightning Location Network (WWLLN) (Dowden *et al.* 2002, Lay *et al.* 2004, Rodger *et al.* 2006) is currently the most prominent example. However, WWLLN is only able to locate major storms accurately, the detection efficiency for cloud to ground lightning events is less than a few percent (Rodger *et al.* 2005). Utilization of WWLLN data to estimate global lightning activity is thus strongly biased to large lightning events.

In the absence of a network that can accurately locate the majority of lightning events worldwide, there is a need for accurate proxy measurements of global lightning activity. Use of a smaller number of receiving sites (1-3) to quantify global lightning activity (but not locate events) and comparison with atmospheric electric field observations was carried out by Füllekrug *et al.* (1999) and Troshichev *et al.* (2004). While energy in the ELF/VLF bands is directly related to global lightning activity, the propagation effects of the Earth-ionosphere waveguide, especially the day *versus* night differences, make this data difficult to interpret. Neither Füllekrug *et al.* (1999) nor Troshichev *et al.* (2004) take propagation effects into account.

A significant issue which recent work has exposed is the specific characteristics of lightning in different regions of the globe. The intensity of lightning events is often categorized by its peak current I_p (the highest electrical current in the return stroke), or the total charge moment $Q\ell$ (total charge transfer multiplied by altitude). In particular, ocean lightning has been shown to be less prevalent than continental lightning but to host the most intense discharges (Biswas and Hobbs 1990). Füllekrug *et al.* (2002) confirm that high peak current discharges are more likely to occur over the ocean and show evidence that such intense ocean discharges are also more likely to be negative rather than positive CG strokes. Chen *et al.* (2008) analyze global distributions of lightning in the context of transient luminous events (TLE) and find that sprites are more often triggered by continental and coastal lightning with the Congo Basin in Subsaharan Africa a key "hot zone" for such observations. In contrast, elve type TLE observations are more prominently produced by ocean lightning with high concentrations in the Carribean Sea, Central and Southwest Pacific Ocean and Indian Ocean. Elves are a product of the electromagnetic pulse (EMP) emitted by lightning strokes (Fukunishi *et al.* 1996) making them an indicator of high peak current of lightning discharges. Sprites, on the other hand, are produced by the quasi-static electric fields (Pasko *et al.* 1997) which are associated with lightning charge moment. Thus, in comparing lightning characteristics

across the globe it seems that African lightning is characterized by relatively higher charge moment, while lightning from the regions of the Pacific and Indian Ocean can be expected to be dominant in the metric of peak current. It is worth noting that such a conclusion is supported by earlier work by Boccippio *et al.* (2000) who utilized OTD and LIS measurements to investigate regional differences in lightning distributions. The authors find that lightning in Africa and in particular the Congo Basin yielded the greatest flash rates with Central America and Southeast Asia (the Maritime Continent) ranking second and third, respectively. However, for mean flash radiance and optical emissions of lightning discharges, ocean regions and Central America clearly supersede the African continent.

Taking into account the disparate properties of global lightning can shed light on the role of these discharges in the global electric circuit, including their effect on diurnal changes in ionospheric potential. Key to making progress in this field is the integration of diverse measurements that have in the past been treated largely in isolation. We present a preliminary study examining ELF/VLF radiation, Schumann resonances, lightning localization, and ionospheric fair weather potential for 14 days during March and May of 2007.

2. SETUP AND METHODOLOGY

2.1 ELF/VLF measurements and analysis

Stanford University operates a network of global receiving sites that record data in the band from 300 Hz to 47 kHz using aircore magnetic field antennas. Cohen *et al.* (2009) provide a description of the receiver hardware. In this study, data from 4 sites are used. The location and abbreviation of each site is given in Table 1. Recordings at each site were made periodically 1 minute out of every 5 minutes or 1 minute out of every 15 minutes for 21 or 23 hours per day depending on the site. For the purpose of estimating lightning

Table 1

Description of receiver stations

Site	Abbreviation	Latitude	Longitude	Observation
Adelaide, Australia	AD	34.32°S	138.46°E	ELF/VLF
Chistochina, USA	CH	62.61°N	144.62°W	ELF/VLF
Palmer, Antarctica	PA	64.05°S	64.77°W	ELF/VLF
Taylor, USA	TA	40.46°N	85.51°W	ELF/VLF
Świder, Poland	SW	52.07°N	21.16°E	E_z
Hornsund, Spitsbergen	HO	72.00°N	15.50°E	E_z
Hylaty, Poland	HY	49.28°N	22.48°E	SR

activity two frequency bands known to be dominated by lightning radiation were chosen for analysis, 9-11 kHz in the VLF band and 310-340 Hz in the ELF band. In this context, further use of the terms VLF and ELF in this work is taken to mean these restricted frequency bands. Hourly amplitude values for each band were calculated at each site by averaging the appropriate frequency spectrum over the synoptic minutes in the hour.

In the initial analysis, the hourly averages were examined directly as was done by Troshichev *et al.* (2004) and it became immediately clear that the day-night propagation effects of the Earth-ionosphere waveguide dominate the variations. Figure 1 shows diurnal averages for 6 days in March 2007 for the ELF and VLF bands recorded at PA as well as maps showing the position of the day-night terminator at various hours during the day. The times corresponding to darkness over the station witness increased amplitudes of ELF/VLF activity. Moreover, the amplitude quickly decreases with the onset of sunrise. The strong influence of the day/night transitions on the observations are due to the higher attenuation of propagating modes by the daytime ionospheric boundary as compared to the nighttime boundary and also reflection of radiation from the terminator boundary itself. Naturally, the propagation effect depends not only on the location of the receiving station with respect to the day-night terminator but also on the location of the lightning

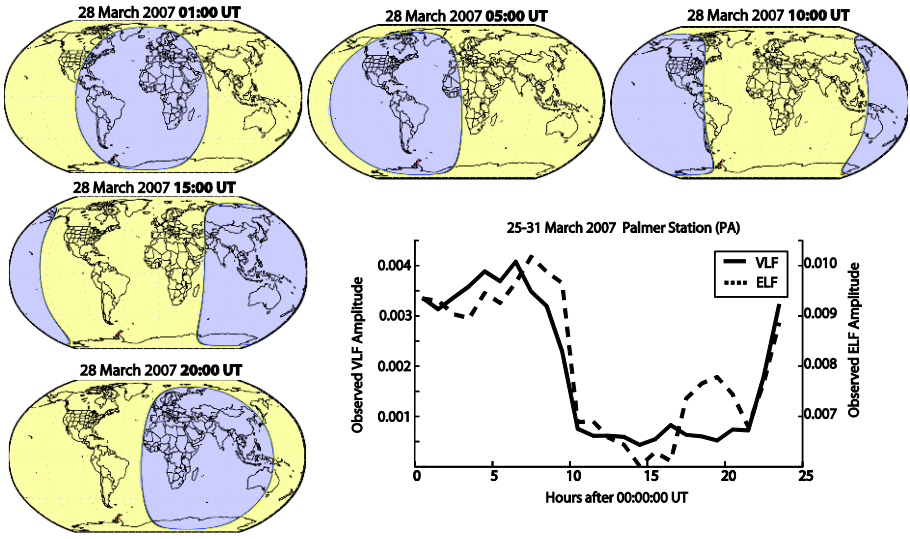

Fig. 1. Maps showing day/night locations at 85 km altitude for various UT times. VLF and ELF hourly amplitudes observed at PA closely correspond to sunrise/sunset conditions at the receiving station. Such local diurnal variations need to be taken into account when interpreting ELF/VLF observations. Colour version of this figure is available in electronic edition only.

radiation source. It is necessary to renormalize the data to account for propagation using an appropriate scaling herein called the ***propagation normalization curve*** in order to make the ELF/VLF observations more accurately reflect global lightning activity. It must be noted that the clear day-night distinction observed at PA results from the specific station location in relation to the worldwide lightning distribution. The effect will in general be different for other stations. Since the propagation effect results from the location and intensity of lightning activity, parameters that we are hoping to evaluate, it at first seems that the problem is intractable without precise knowledge of the location and intensity of each lightning event. However, it is possible to use the expected location and intensity of lightning events to determine an effective propagation normalization curve for each site. To this end, we utilize the database compiled from the LIS instrument which gives the average worldwide distribution of lightning events for each day of the year, based on a 5-year average.

To calculate a propagation normalization curve for each site, the LIS average flash rate for each latitude, longitude location is used as a measure for lightning intensity and the propagation attenuation to the receiver site in question is calculated as a function of Universal Time. The attenuation calculation is carried out separately for the ELF and VLF bands using published frequency dependent daytime and nighttime attenuation rates (Watt 1967, p. 338). For the VLF band the daytime and nighttime attenuation rates used are –5 dB/1000 km and –3 dB/1000 km, respectively, and for the ELF band the respective rates are –11 dB/1000 km and –5 dB/1000 km. Only locations within 6000 km of the receiver site were taken into account since lightning activity within this distance makes the dominant contribution to observed ELF/VLF amplitude. In addition to daytime and nighttime attenuation due to propagation distance, an attenuation coefficient was applied for propagation paths that crossed the day-night terminator. If the daytime and nighttime paths are modeled as waveguides with different effective heights, this terminator attenuation factor represents the coupling coefficient between the two waveguides. Theoretical work by Wait (1981, p. 147) and comparison of VLF measurements in the United States with localizations from the National Lightning Detection Network show that the attenuation for a typical day-night transition is –1 dB, while for a night-day transition is –5 dB.

The calculated curves were subsequently normalized to their maximum value. The resulting curves for all 4 ELF/VLF sites for 20 May 2007 are shown in Fig. 2. The curves in Fig. 2 should be interpreted as normalized expected activity in the ELF/VLF bands due to global lightning. The expected activity curves for the PA site are seen to resemble closely the observed ELF/VLF activity shown in Fig. 1 and testify to the correct modeling of daytime *versus* nighttime propagation effects. Inversion of the expected

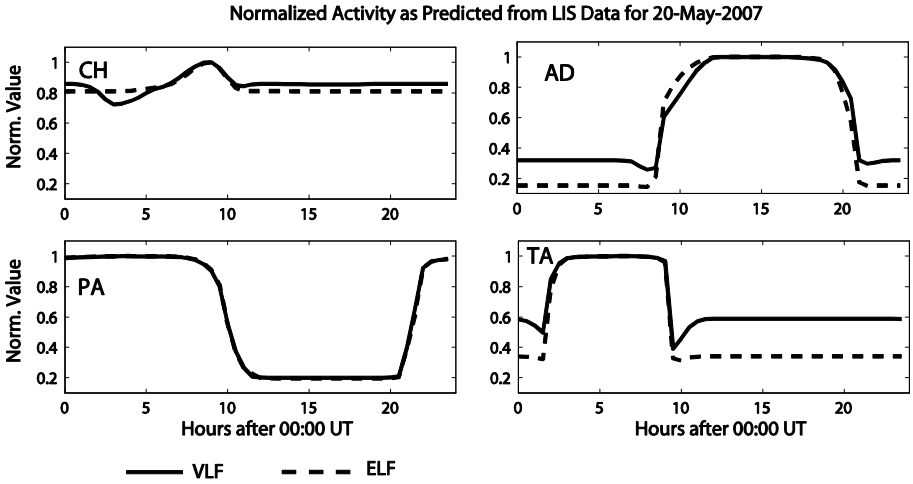

Fig. 2. Normalized expected amplitudes in the ELF and VLF bands for four receiving sites based on LIS flash rate and day/night attenuation of propagation as described in the text.

activity curves yields a propagation normalization curve that effectively removes the geography and time dependent propagation effects at each site. Scaling with the propagation normalization curve allows lightning data across sites to be compared directly. The validity of the technique lies in the application of well established distribution averages provided by LIS to remove geography specific variations in daily measurements.

Armed with the appropriate propagation normalization curves we use three to four globally spaced sites to estimate global lightning activity. We choose sites spread geographically so as to sample the three major global lightning centers of Africa, Asia/Oceania and the Americas. Despite having already addressed global propagation effects, the geographic spread of multiple receivers allows the inclusion of distant lightning events whose ELF/VLF signatures would otherwise be lost to the noise floor after long distance propagation. The lightning activity as observed and normalized for propagation at each site is then summed across the three (or four) stations using an $L2$-norm to yield a global lightning activity curve as a function of Universal Time. An $L2$-norm is the square root of the sum of the squares of all components. Although we strongly believe that propagation scaling technique enables more accurate interpretation of the ELF/VLF data, we additionally show the raw (unscaled) values for the purposes of comparison with previous works. Examples of ELF/VLF data can be seen in Figs. 7-12.

2.2 Schumann resonance observations

Measurements of Schumann resonances (SR) were performed at the HY site using two channel magnetic field observations oriented in the north-south (NS) and east-west (EW) directions. A challenge in lightning activity estimations from SR observations is the simultaneous existence and interaction of standing and propagating waves in the spherical shell Earth-ionosphere cavity. To derive lightning activity from SR observations we use the technique of modal decomposition described by Kułak *et al*. (2006). This technique is based on the expression of the 4-60 Hz spectrum by an asymmetric function. The observed power spectrum of frequency f is fitted to the following formula (Nieckarz *et al.* 2009):

$$\left|B(f)\right|^2 = s + \frac{z}{f^{\alpha}} + \sum_{k=1}^{\infty} \frac{p_k\left[1+\varepsilon_k(f-f_k)\right]}{(f-f_k)^2 + \Gamma_k^2/2}\ , \tag{1}$$

where p_k describes the power parameter of the k-th resonance mode, ε_k is the asymmetry parameter of the k-th resonance mode. The parameters f_k and Γ_k are the resonance frequency and resonance width, respectively. White noise power is represented with amplitude s and pink noise ($1/f^{\alpha}$) with amplitude s. The spectrum from each antenna is fitted to eq. (1) and lightning activity is computed by summation over the power parameters p_k

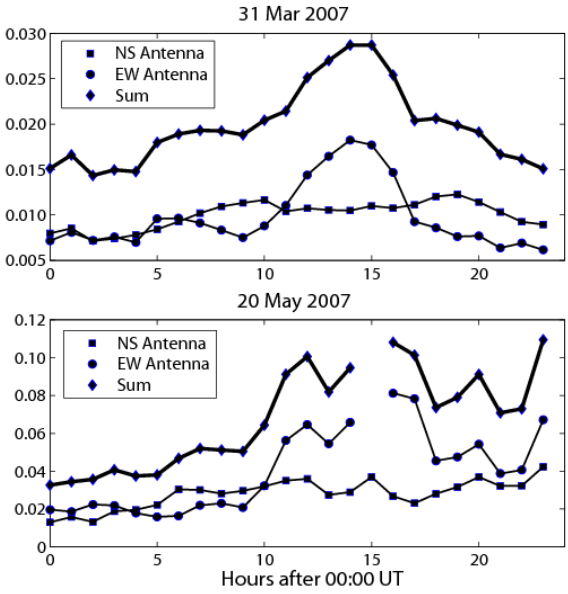

Fig. 3. Lightning activity as derived from measurements of Schumann resonances. NS and EW refer to observations of magnetic field in the north-south and east-west directions.

$$SR_{NS} = \sum_{1}^{7} p_{NS,k} \qquad SR_{EW} = \sum_{1}^{7} p_{EW,k} \,. \tag{2}$$

Figure 3 shows SR derived lightning activity for 31 March and 20 May 2007 which were computed using 15 minute spectra.

2.3 Atmospheric electric field observations

The fair weather atmospheric electric field (vertical electric field measured at the ground) E_z is observed at mid-latitude at site SW and polar latitude at HO using a radioactive collector (Am245) with heated insulator and simultaneously rotating dipole field mill (Kubicki 2008). The sensors are installed 2 m above the ground surface with measurements collected at 10 second resolution. Observations of E_z at SW have been taken over many decades and are well characterized in terms of seasonal and diurnal variation. Figure 4a, adapted from Fig. 5 of Kubicki *et al.* (2007), shows the normalized daily variation of electric field over select summer and winter days during the years 1965-2000. While the winter variation can be seen to match the classic Carnegie curve, the summer variation exhibits two maxima at 06:00-08:00 UT and 17:00-20:00 UT, as influenced by summer afternoon convective mixing typical of land stations (Kubicki *et al.* 2007, Chalmers 1967, p. 162-169). Figure 4b shows the winter and summer air conductivity averaged over the same period. Since the conductivity and electric field exhibit an inverse relationship only for the late evening and night hours, diurnal observations of E_z at SW can be interpreted as measures of global ionospheric potential (Kubicki *et al.* 2007). Nevertheless, as the susceptibility of land E_z measurements to local influences is well documented (Williams 2009), it is important to interpret the data from SW in the context of the characteristics of observations from this station.

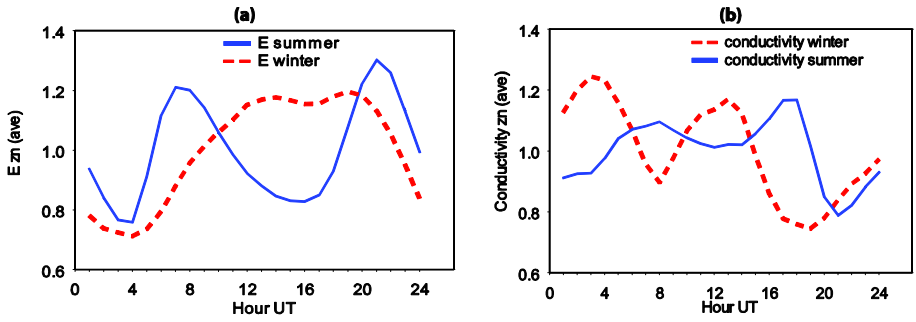

Fig. 4. The normalized daily variations of electric field (a) and conductivity (b), normalized and averaged values, over selected days in winter (89) and summer (289) at Świder from 1965 to 2000. Reproduced from Kubicki *et al.* (2007). Colour version of this figure is available in electronic edition only.

Table 2

Observation dependencies

Observation	Measurement
VLF	$\|I_p\| F_r$
ELF	$<\|Q\ell\|, \|I_p\|> F_r$
SR	$\|Q\ell\| F_r$
WWLLN	αF_r
E_z	Q_{tot}

A cohesive interpretation of the diverse observations presented above calls for identifying the measurement dependencies in the context of the global electric circuit. A listing of the observation dependencies is presented in Table 2 where we show lightning related observables in terms of the true global flash rate F_r. Radiation observed in the VLF band is a measure of the product of the flash rate and the peak current I_p of each strike. On the other end of the spectrum, the less than 60 Hz radiation of the Schumann resonances is largely a measure of the charge moment $Q\ell$ of lightning discharges. In this context, the ~300 Hz ELF observations are an intermediate and a proxy for both peak current and charge moment. For lightning detection networks, of which WWLLN is an example, the observable is the flash rate scaled by the detection efficiency α, which will depend on the location of receiving stations and the specifics of the algorithm employed. On global scales, the value of α for WWLLN does not exceed 5% (of cloud to ground lightning) (Rodger *et al.* 2005). In the case where local effects have been minimized, E_z is a measure of the global ionospheric potential, which depends on the total charge separation Q_{tot} between the Earth and the ionosphere. The disparate properties of lightning discharges in the different regions of the Earth have already been described above. Given such regional differences, it is expected that individual lightning regions will have dissimilar effects on the different instruments. For example, the high peak currents of lightning associated with the oceans and the maritime continent are expected predominantly to influence VLF observations, while the high charge moment strikes of the Congo Basin can be expected to be observed in Schumann resonance measurements.

3. OBSERVATIONS AND ANALYSIS

In this study we analyze fourteen days of fair weather at SW, seven days each in the months of March and May 2007. During this time, ELF/VLF data were available from at least 3 sites and SR data were obtained for 31 March

and 20 May. The days of the study coincided with fair weather conditions at HO on 31 March. For most days of the study we note only minimal correlation between the ELF/VLF and SR lightning diagnostics and E_z observations. The general behavior of the diurnal E_z curve was seen to follow the summer average shown in Fig. 4 with notable exceptions discussed below.

3.1 Data from 31 March and 20 May

The days 31 March and 20 May were those for which the most measurements were available. The SR derived lightning activity for both of these days, as shown in Fig. 3, is found to exhibit a central peak between 10:00-18:00 UT, which is classically associated with lightning activity in the African sector as established by thunder days (Whipple and Scrase 1936). The E_z observations for these days shown in Fig. 5 are not seen to be correlated with the SR measurements. It is worth mentioning a recent study by Nieckarz *et al.* (2009) who examined two years of fair weather E_z data from SW with SR data using the identical receiving station (HY) and technique as we use here. The calculated correlation coefficients (between E_z and SR) spanned a wide range including both positive and negative values and notably a few days of very high positive correlations of 0.9. The SR diurnal

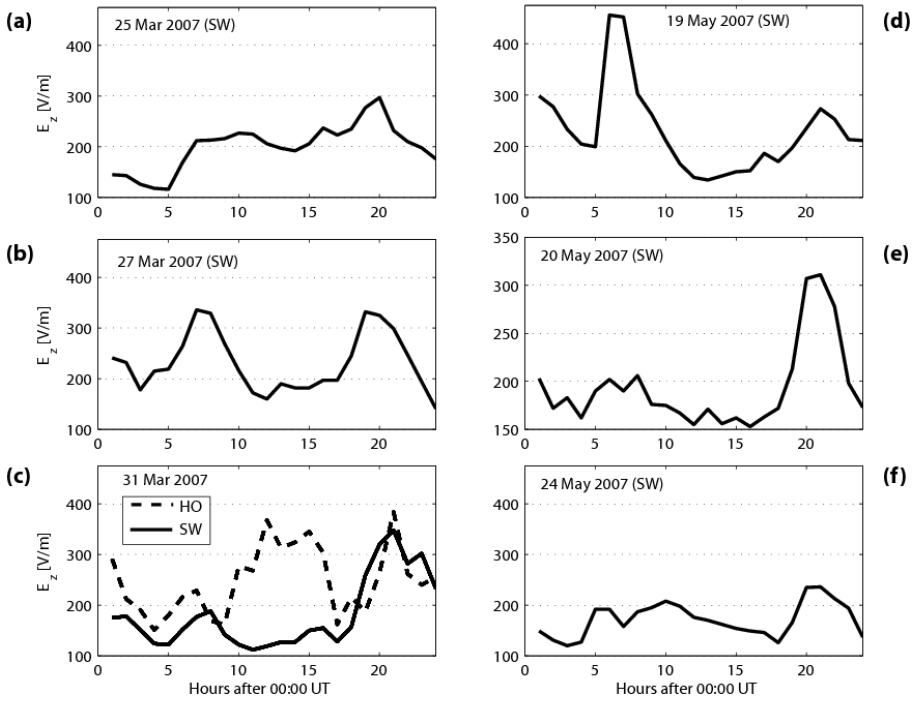

Fig. 5. Observations of atmospheric electric field E_z.

lightning activity averaged over the two year period exhibited the same general characteristics of a dominant late afternoon peak that is seen in Fig. 3. Hence, the observations presented here as well of those of Nieckarz *et al.* (2009) support the notion that the SR observations are more sensitive to the high charge moments and high flash rates associated with African lightning relative to other global regions. An examination of data from the WWLLN network for 20 May 2007 corroborates this view. Figure 6 shows the number of geolocated flashes from the WWLLN network for 20 May 2007 for the world (top panels) and also for global regions divided by longitude to represent roughly the three major lightning centers of Africa, Asia (Maritime Continent), and the Americas. The left panels in Fig. 6 show the number of flashes when an observation restriction of at least 7 receiving stations is imposed, while the right panels show data for a less strict criterion of 5 minimum stations. It is clear that increasing the observation station requirement causes the number of geolocated flashes attributed to the African sector to decrease more substantially than for the other two regions and thereby changes the shape of the diurnal world total flash detection curve. This high sensitivity of geolocation in the African sector to the number of receiving stations is likely caused by a small number of WWLLN stations near Africa

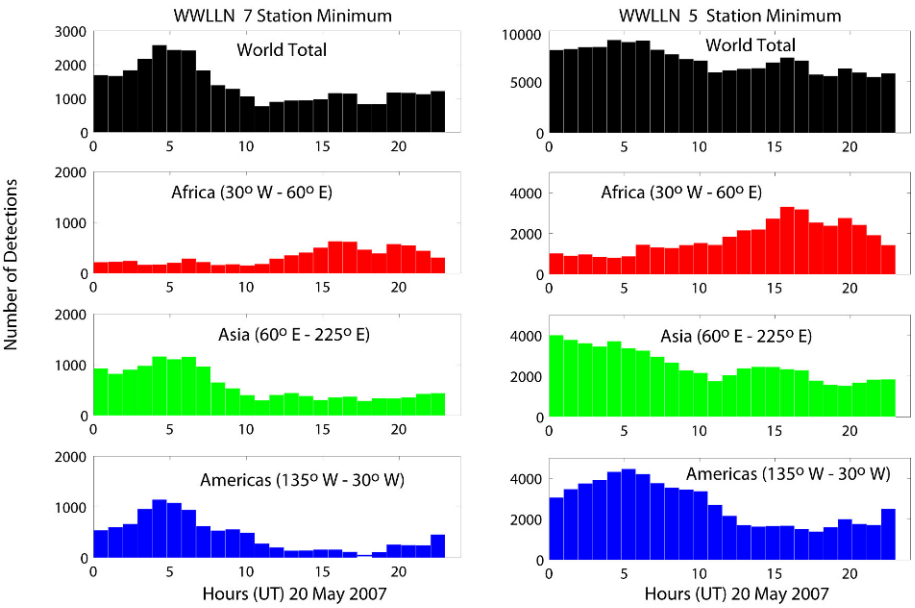

Fig. 6. Lightning location data from the WWLLNN network. Flashes on the left (right) hand side were observed by at least 7(5) stations. Colour version of this figure is available in electronic edition only.

but can also result from the relatively lower peak current of lightning in this region as discussed in Section 1. Since WWLLN receivers monitor the VLF band (6-22 kHz), the network is most sensitive to discharges with high peak currents. We note that the general diurnal distribution of African lightning flashes located by WWLLN is in agreement with the SR measurements for 20 May. However, neither the WWLLN network on this day nor on other days examined in May 2007 does exhibit the dominance of the African sector for flash rates as has been reported elsewhere (Boccipio *et al.* 2000). Although a powerful tool, the WWLLN network is not yet able to quantify lighting on a global scale effectively.

Figures 9 and 11 show the ELF/VLF data for 31 March and 20 May in the unscaled raw amplitude form (left panels) and the propagation scaled form (right panels) described in Section 2.1. The main difference in the VLF data between these two days is that on 20 May activity is dominated by the AD station while for 31 March the TA and CH stations provide contributions of equal magnitude. This difference would suggest elevated Australian/Asian lightning on 20 May. Both days also exhibit a final late day peak in activity. In the scaled ELF data this peak occurs around 21:00-22:00 UT on both days. In the VLF data, however, the peak occurs earlier (19:00 UT) on 20 May even though on both days it is largely due to observations at PA. Looking closely at ELF/VLF data from different stations it appears that the scaled ELF amplitude observed at PA most closely correlates to the SR measurements. In particular, the three peaks at 12:00, 15:00, and 19:00-20:00 UT on 20 May are present in both datasets. The correspondence is likely due to the fact that both these measurements are most sensitive to the African lightning flashes. For the ELF PA measurement the sensitivity is based both on location and higher charge moment of these flashes.

Figure 5c shows E_z curves from both HO and SW recorded on 31 March. Outside of the hours 10:00-16:00 UT, the two curves show good agreement of amplitude and behavior. However, for the 10:00-16:00 UT period, the observations at HO show an elevated E_z not observed at SW. In this context, the observations at HO more clearly exhibit the African center prominent in the SR observations and can be even said to be a good match to the scaled ELF/VLF data (peaks at 12:00, 15:00, and 21:00 UT) on this day. Although it seems that the E_z values observed at HO on 31 March might be driven by global lightning, it is important to keep in mind that atmospheric electric field observations at polar latitudes are also heavily influenced by magnetospheric processes including auroral precipitation and solar wind (Michnowski 1998). Unfortunately, fair weather days at HO were limited during the present study but will be investigated more thoroughly in the future.

3.2 ELF/VLF data from 25 March *versus* 27 March

Figures 7 and 8 show ELF/VLF data from 25 and 27 March, respectively. The data for 25 March stand out in that uncharacteristically strong VLF activity is observed at the CH station. This is most clearly seen in the scaled VLF data (upper right panel of Figure 7 where a 3 hour peak centered at 15:00 UT is visible). No such peak is observed in data from the closest consecutive day (27 March, Fig. 8) nor in any other days of the study (Figs. 7-12). Moreover, no enhancement is observed in the ELF data at this time (Fig. 7, lower right panel). Given the location of the CH station in Alaska and the prevalence of radiation in VLF over the ELF band, it is likely that the observations result from unusually high activity of lightning over the Pacific Ocean that is known to yield very high peak currents (Boccippio *et al.* 2000, Füllekrug *et al.* 2002). Examination of the E_z data for this time also shows an unusual trend. As can be seen in Fig. 5a, E_z observed at SW does not exhibit the mid day drop as on the other days of the study and in the average summer diurnal variation (Fig. 4a). The value of E_z remains close to 200 V/m from 05:00-18:00 UT. It is possible that intense lightning in the Pacific Ocean is causing the global ionospheric potential to remain elevated during this particular time.

3.3 ELF/VLF data from 19 May *versus* 20 May

On 19 May the E_z data exhibit a very strong peak of up to 450 V/m at 06:00-07:00 UT. Furthermore, the second peak at 22:00 UT is much subdued relative to other days where the times around 20:00-22:00 UT normally dominate the diurnal behavior. On the following day, 20 May, the situation is reversed in that the electric field from 05:00-08:00 UT is reduced and the second peak at 20:00-22:00 UT is dominant. The ELF/VLF data for these days are shown in Figs. 10 and 11. The total ELF/VLF activity curves do not show correlation with either day and it is more useful to examine observations from the individual stations. Most notably, the scaled VLF data from PA on 19 May does not exhibit the prominent late day peak that is seen on 20 May and also on 25 March and 31 March. This peak seems to be a recurring feature in the VLF data from PA, although it is not observed in the ELF band. On 19 May there is also considerably more ELF and VLF activity observed at TA in the 00:00-08:00 UT hours as compared to 20 May.

3.4 Multi-day averages

Figure 13 shows averages of ELF/VLF and E_z for the seven days in March and seven days in May separated by month. The ELF/VLF data were computed using the three sites, AD, CH and PA, which recorded data on all days of the study. The averaged ELF and VLF data for March and the VLF data for May exhibit resemblance to the classic Carnegie curve (Whipple and

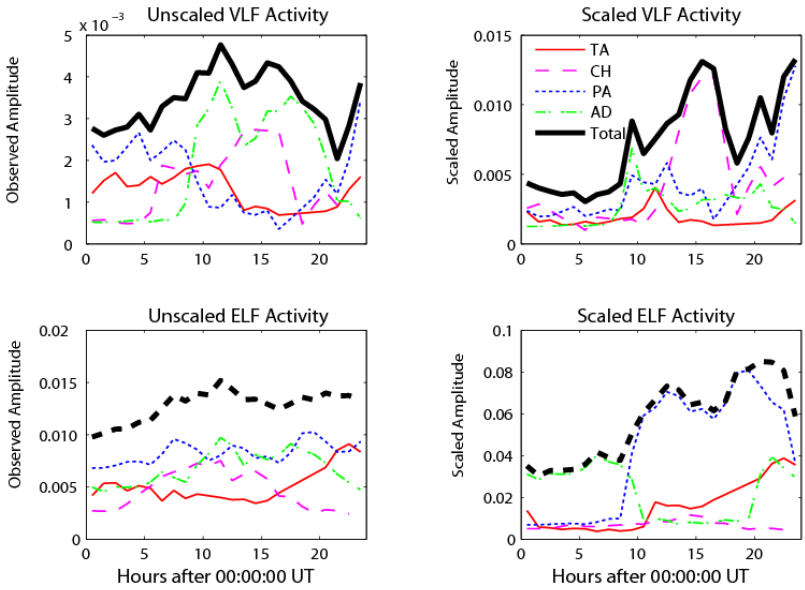

Fig. 7. ELF/VLF activity for 25 March 2007 observed at sites AD, CH, PA, and TA. Plots on the left show observations without taking into account propagation effects. The plots on the right are scaled by site specific propagation normalization curves. Colour version of this figure is available in electronic edition only.

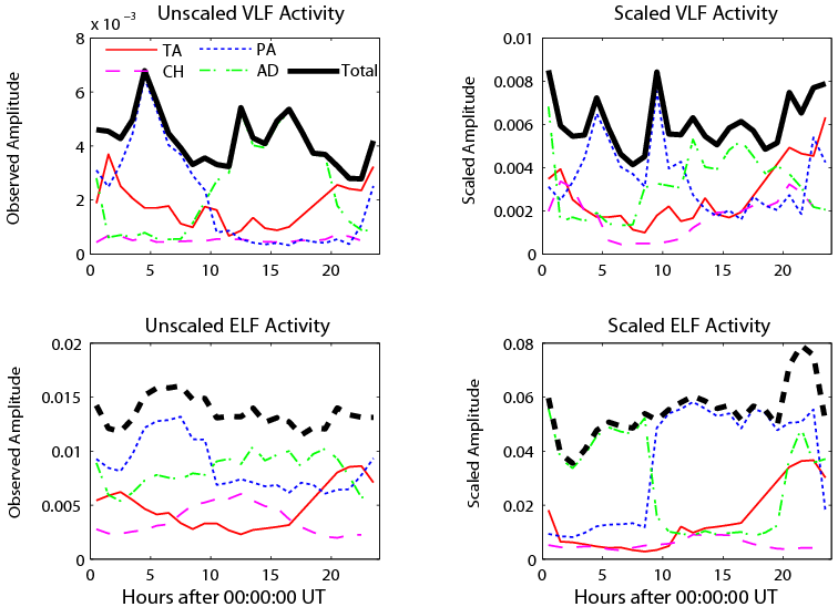

Fig. 8. Same as Fig. 7 but for 27 March 2007. Colour version of this figure is available in electronic edition only.

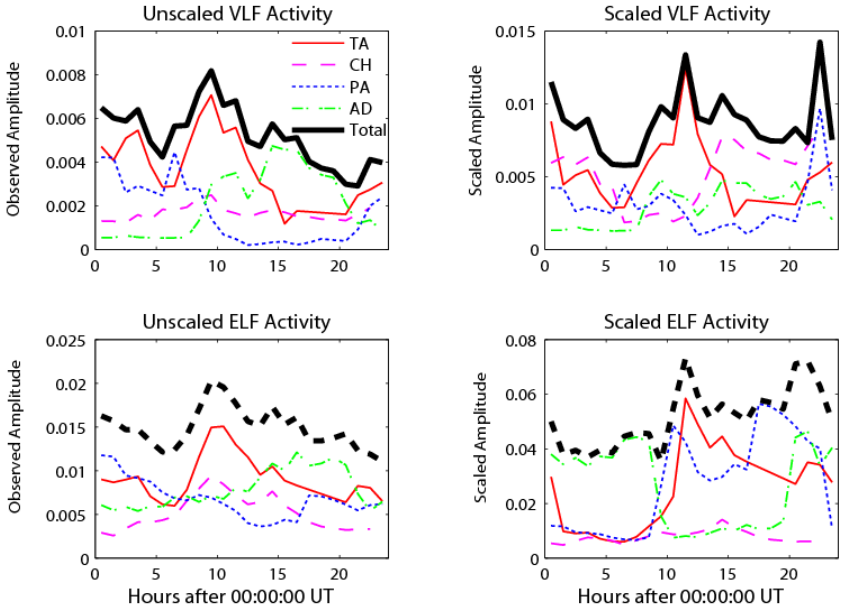

Fig. 9. Same as Fig. 7 but for 31 March 2007. Colour version of this figure is available in electronic edition only.

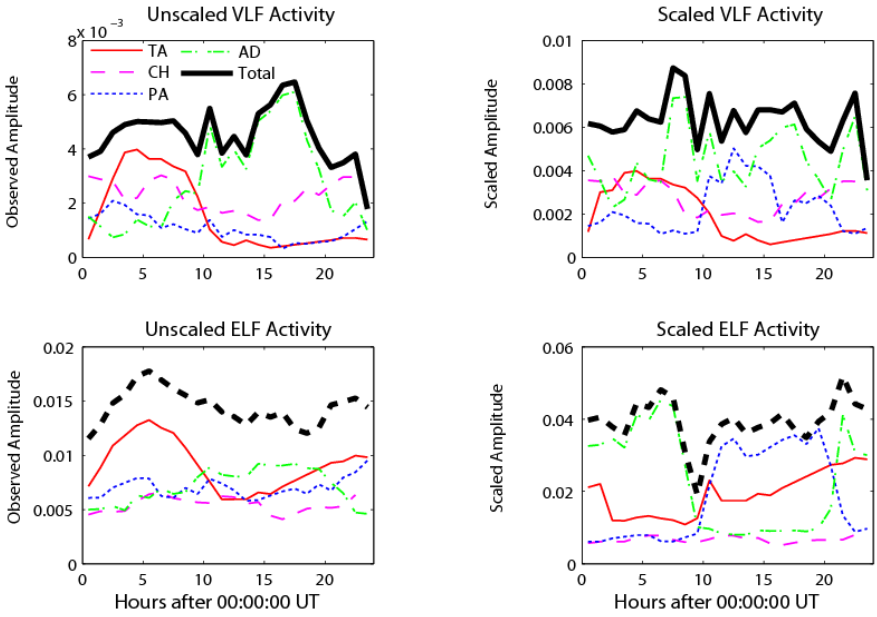

Fig. 10. Same as Fig. 6 but for 19 May 2007. Colour version of this figure is available in electronic edition only.

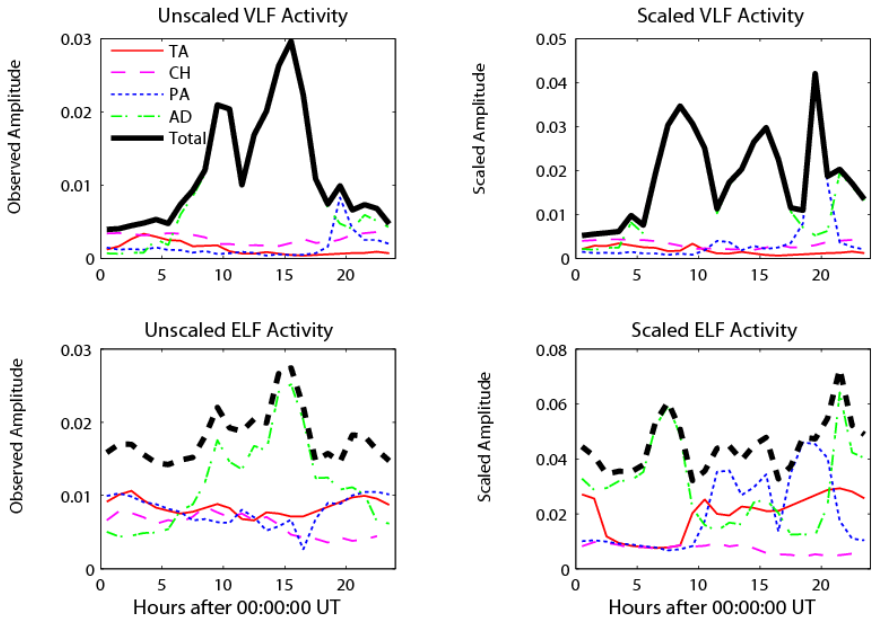

Fig. 11. Same as Fig. 7 but for 20 May 2007. Colour version of this figure is available in electronic edition only.

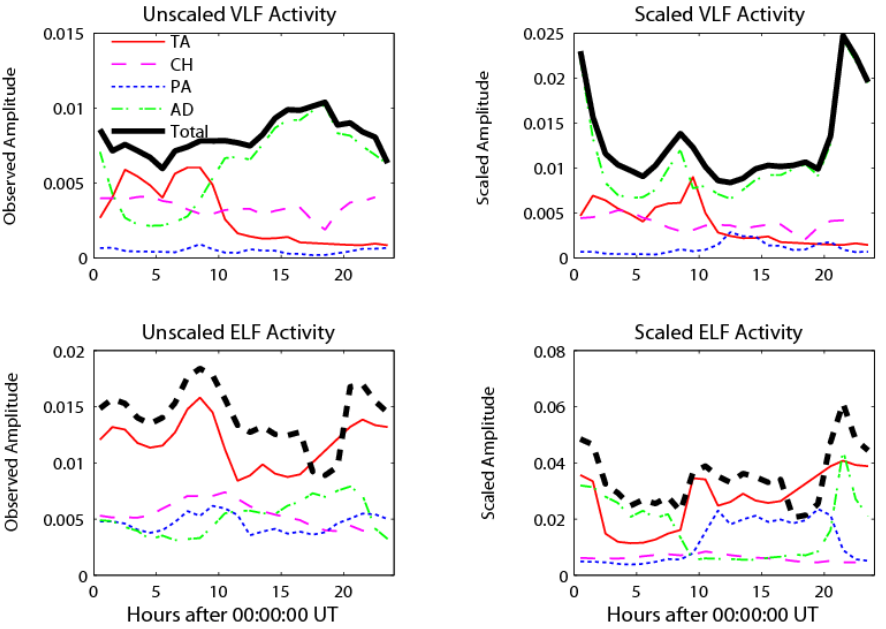

Fig. 12. Same as Fig. 7 but for 24 May 2007. Colour version of this figure is available in electronic edition only.

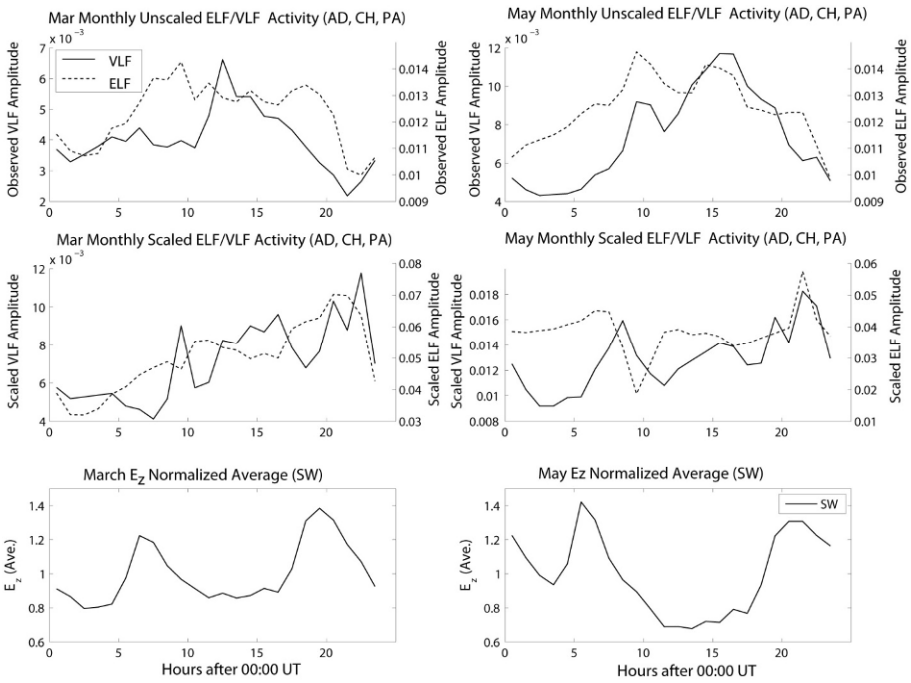

Fig. 13. Multi-day fair weather averages for ELF/VLF estimates of global lightning activity and atmospheric electric field observed at SW.

Scrase 1936). In particular, in the VLF data for March it is possible to identify three peaks of storm activity corresponding to the three global lightning centers. Looking at the scaled VLF data the central peak (12:00-15:00 UT), normally associated with lightning in the African sector, is lower for the days in May as compared to March. The averaged E_z curves are similar to the long term averages shown in Fig. 4a with two dominant peaks at 06:00-07:00 UT and 18:00-21:00 UT. For the March days the values around the first peak are lower than the second peak, but for the May days the situation is reversed. We note that the scaled ELF amplitudes are relatively enhanced during the hours of the first E_z peak in May as compared to March. Likewise, the VLF raw amplitudes (unscaled panels) are 20-30% higher in May than in March. The electric field during the hours 10:00-16:00 UT is also lower in May than in March, which may be a result of the lower average VLF activity during this time, as noted above.

4. SUMMARY AND DISCUSSION

We have analyzed widely spaced ELF, VLF, SR and E_z for select days in March and May 2007. A theme of our work has been the integration of different globally spaced measurements and investigating the regional differ-

ences of lightning discharges in the context of the global electric circuit. We have introduced a method of mitigating propagation effects in ELF/VLF observations that is based on well established day/night propagation models and lightning averages from the LIS instrument. The propagation scaling method is effective in providing an estimate of global lightning activity using three or more geographically spaced stations. Although looking at ELF/VLF amplitudes from a small number of stations does not yield precise location information on the radiation source, such measurements do capture important lightning discharge features that are lost to the algorithms of lightning location networks such as WWLLN.

We find that SR lightning measurements as well as ELF observations at PA are most sensitive to lightning in sub-Saharan Africa. We believe that this is related to the characteristic high charge moment ($Q\ell$) of these discharges as compared to other lightning sectors. On the other hand, the high peak current (I_p) of ocean lightning is found to predominantly influence VLF observations. Although our preliminary dataset is not large enough to be statistically significant, our observations suggest that the global ionospheric potential may be more sensitive to high peak current lightning discharges. A future study has been planned that will encompass a larger number of fair weather days and ELF/VLF measurements. Although the polarization of the lightning discharges determines whether they will increase or decrease the ionospheric potential and is therefore of critical importance, our observations do not currently allow us to distinguish between positive and negative cloud to ground discharges. A relevant issue is the dominance of American lightning over African lightning in relation to the Carnegie curve. Kartalev *et al*. (2006) propose that the location of lightning in relation to the magnetic dip equator plays an important role while other workers have suggested that the answer lies in electric rain showers which are dominant in South America (Williams and Sátori 2004). Our study suggests that the disparate discharge characteristics of lightning in different regions should also be taken into account in addressing this question. Moreover, long term ELF/VLF observations with globally spaced receivers, as presented here, can be used to complement the world lightning distributions obtained from satellites. Although the space borne optical observations have greatly enhanced understanding of the global lightning, these measurements are biased by the additional variable of atmospheric opacity at optical wavelengths which can also exhibit regional variation.

Acknowledgments. This work is an outgrowth of collaboration between Stanford University and the Polish Academy of Sciences initiated under the International Heliophysical Year 2007-2009 and the associated distribution of AWESOME ELF/VLF receivers (Sherrer *et al*. 2008).

References

Biswas, K.R., and P.V. Hobbs (1990), Lightning over the Gulf Stream, *Geophys. Res. Lett*. **17**, 7, 941-943, DOI: 10.1029/GL017i007p00941.

Boccippio, D.J., S.J. Goodman, S. Heckman (2000), Regional differences in tropical lightning distributions, *J. Appl. Meteorol.* **39**, 12, 2231-2248, DOI: 10.1175/1520-0450(2001)040<2231:RDITLD>2.0.CO;2.

Chalmers, J.A., (1967), *Atmospheric Electricity*, 2nd ed., Pergamon Press, Oxford – New York, 515 pp.

Chen, A.B., C.-L. Kuo, Y.-J. Lee, H.-T. Su, R.-R. Hsu, J.-L. Chern, H.U. Frey, S.B. Mende, Y. Takahashi, H. Fukunishi, Y.-S. Chang, T.-Y. Liu, and L.-C. Lee (2008), Global distributions and occurrence rates of transient luminous events, *J. Geophys. Res.* **113**, A08306, DOI: 10.1029/2008JA013101.

Christian, H.J., R.J. Blakeslee, D.J. Boccippio, W.L. Boeck, D.E. Buechler, K.T. Driscoll, S.J. Goodman, J.M. Hall, W.J. Koshak, D.M. Mach, and M.F. Stewart (2003), Global frequency and distribution of lightning as observed from space by the Optical Transient Detector, *J. Geophys. Res*. 108, D1, 4005, DOI: 10.1029/2002JD002347.

Cohen, M.B., U.S. Inan, and E. Paschal (2009), Sensitive broadband ELF/VLF radio reception with the AWESOME instrument, *IEEE Trans. Geosci. Remote Sens.* **48**, 1, 3-17, DOI: 10.1109/TGRS.2009.2028334.

Dowden, R.L, J.B. Brundell, and C.J. Rodger (2002), VLF lightning location by time of group arrival (TOGA) at multiple sites, *J. Atmos. Sol.-Terr. Phys.* **64**, 7, 817-830, DOI: 10.1016/S1364-6826(02)00085-8.

Fukunishi, H., Y. Takahashi, M. Kubota, K. Sakanoi, U.S. Inan, and W.A. Lyons (1996), Elves: Lightning-induced transient luminous events in the lower ionosphere, *Geophys. Res. Lett.* **23**, 16, 2157-2160, DOI: 10.1029/96GL01979.

Füllekrug, M., and A.C. Fraser-Smith (1996), Further evidence for a global correlation of the Earth-ionosphere cavity resonances, *Geophys. Res. Lett.* **23**, 20, 2773-2776, DOI: 10.1029/96GL02612.

Füllekrug, M., A.C. Fraser-Smith, E.A. Bering, and A.A. Few (1999), On the hourly contribution of global cloud-to-ground lightning activity to the atmospheric electric field in the Antarctic during December 1992, *J. Atmos. Sol.-Terr. Phys*. **61**, 10, 745-750, DOI: 10.1016/S1364-6826(99)00031-0.

Füllekrug, M., C. Price, Y. Yair, and E.R. Williams (2002), Intense oceanic lightning, *Ann. Geophys*. **20**, 1, 133-137, DOI: 10.5194/angeo-20-133-2002.

Kartalev, M.D., M.J. Rycroft, M. Füllekrug, V.O. Papitashvili, and V.I. Keremidarska (2006), A possible explanation for the dominant effect of South American thunderstorms on the Carnegie curve, *J. Atmos. Sol.-Terr. Phys.* **68**, 3-5, 457-468, DOI: 10.1016/j.jastp.2005.05.012.

Kubicki, M. (2008), Atmospheric electricity research at the Institute of Geophysics in the years 2006-2007, *Publs. Inst. Geophys. Pol. Acad. Sc.* **D-72**, 403, 105-110.

Kubicki, M., S. Michnowski, and B. Mysłek-Laurikainen (2007), Seasonal and daily variations of atmospheric electricity parameters registered at the Geophysical Observatory at Świder (Poland) during 1965-2000, Proc. 13th Int. Confer. on Atmospheric Electricity, ICAE 2007, Beijing, 50-54.

Kułak, A., J. Młynarczyk, S. Zięba, S. Micek, and Z. Nieckarz (2006), Studies of ELF propagation in the spherical shell cavity using a field decomposition method based on asymmetry of Schumann resonance curves, *J. Geophys. Res*. **111**, A10304, DOI: 10.1029/2005JA01142.

Lay, E.H., R.H. Holzworth, C.J. Rodger, J.N. Thomas, O. Pinto Jr., and R.L. Dowden (2004), WWLL global lightning detection system: Regional validation study in Brazil, *Geophys. Res. Lett*. **31**, L03102, DOI: 10.1029/2003GL 018882.

Michnowski, S. (1998), Solar wind influences on atmospheric electricity variables in polar regions, *J. Geophys. Res*. **103**, D12, 13939-13948, DOI: 10.1029/ 98JD01312.

Nieckarz, Z., A. Kułak, S. Zięba, M. Kubicki, S. Michnowski, and P. Barański (2009), Comparison of global storm activity rate calculated from Schumann resonance background components to electric field intensity E_{0Z}, *Atmos. Res.* **91**, 2-4, 184-187, DOI: 10.1016/j.atmosres.2008.06.006.

Pasko, V.P., U.S. Inan, and T.F. Bell (1997), Sprites as evidence of vertical gravity wave structures above mesoscale thunderstorms, *Geophys. Res. Lett.* **24**, 14, 1735-1738, DOI: 10.1029/97GL01607.

Rodger, C.J., J.B. Brundell, and R.L. Dowden (2005), Location accuracy of VLF World-Wide Lightning Location (WWLL) network: Post-algorithm upgrade, *Ann. Geophys.* **23**, 2, 277-290, DOI: 10.5194/angeo-23-277-2005.

Rodger, C.J., S. Werner, J.B. Brundell, E.H. Lay, N.R. Thomson, R.H. Holzworth, and R.L. Dowden (2006), Detection efficiency of the VLF World-Wide Lightning Location Network (WWLLN): Initial case study, *Ann. Geophys.* **24**, 12, 3197-3214, DOI: 10.5194/angeo-24-3197-2006.

Rycroft, M.J., S. Israelsson, and C. Price (2000), The global atmospheric electric circuit, solar activity and climate change, *J. Atmos. Sol.-Terr. Phys.* **62**, 17-18, 1563-1576, DOI: 10.1016/S1364-6826(00)00112-7.

Rycroft, M.J., A. Odzimek, N.F. Arnold, M. Füllekrug, A. Kułak, and T. Neubert (2007), New model simulations of the global atmospheric electric circuit driven by thunderstorms and electrified shower clouds: The roles of lightning and sprites, *J. Atmos. Sol.-Terr. Phys.* **69**, 17-18, 2485-2509, DOI: 10.1016/j.jastp.2007.09.004.

Scherrer, D., M.B. Cohen, T. Hoeksema, U.S. Inan, R. Mitchell, and P. Scherrer (2008), Distributing space weather monitoring instruments and educational

materials worldwide for IHY 2007: The AWESOME and SID project, *Adv. Space Res.* **42**, 11, 1777-1785, DOI: 10.1016/j.asr.2007.12.013.

Tinsley, B.A., and L. Zhou (2006), Initial results of a global circuit model with variable stratospheric and tropospheric aerosols, *J. Geophys. Res.* **11**, D16205, DOI: 10.1029/2005JD006988.

Troshichev, O.A., A. Frank-Kamenetsky, G. Burns, M. Füllekrug, A. Rodger, and V. Morozov (2004), The relationship between variations of the atmospheric electric field in the southern polar region and thunderstorm activity, *Adv. Space Res.* **34**, 8, 1801-1805, DOI: 10.1016/j.asr.2003.07.063.

Wait, J.R. (1981), *Lectures on Wave Propagation Theory*, Pergamon Press, New York.

Watt, A.D. (1967), *VLF Radio Engineering*, Pergamon Press, New York.

Whipple, F.J.W., and F.J. Scrase (1936), Point discharge in the electric field of the earth, *Geophysical Memoirs of London VII* **68**, 1-20.

Williams, E.R. (2009), The global electric circuit: A review, *Atmos. Res.* **91**, 2-4, 140-152, DOI: 10.1016/j.atmosres.2008.05.018.

Williams, E.R., and G. Sátori (2004), Lightning, thermodynamic and hydrological comparison of the two tropical continental chimneys, *J. Atmos. Sol.-Terr. Phys.* **66**, 13-14, 1213-1231, DOI: 10.1016/j.jastp.2004.05.015.

Wilson, C.T.R. (1921), Investigations on lightning discharges and on the electric field of thunderstorms, *Philos. Trans. Roy. Soc. Lond. A* **221**, 73-115.

Received 12 April 2010
Received in revised form 21 June 2010
Accepted 29 June 2010